Fusion Science and Technology

ISSN: 1536-1055 (Print) 1943-7641 (Online) Journal homepage: https://www.tandfonline.com/loi/ufst20

Integrated Plasma Control in DIII-D

D. A. Humphreys, R. D. Deranian, J. R. Ferron, A. W. Hyatt, R. D. Johnson, R. R. Khayrutdinov, R. J. La Haye, J. A. Leuer, B. G. Penaflor, J. T. Scoville, M. L. Walker & A. S. Welander

To cite this article: D. A. Humphreys, R. D. Deranian, J. R. Ferron, A. W. Hyatt, R. D. Johnson, R. R. Khayrutdinov, R. J. La Haye, J. A. Leuer, B. G. Penaflor, J. T. Scoville, M. L. Walker & A. S. Welander (2005) Integrated Plasma Control in DIII-D, Fusion Science and Technology, 48:2, 1249-1263, DOI: 10.13182/FST05-A1075

To link to this article: https://doi.org/10.13182/FST05-A1075

INTEGRATED PLASMA CONTROL IN DIII-D

D. A. HUMPHREYS,* R. D. DERANIAN, J. R. FERRON, A. W. HYATT, R. D. JOHNSON,
R. R. KHAYRUTDINOV,† R. J. LA HAYE, J. A. LEUER, B. G. PENAFLOR,
J. T. SCOVILLE, M. L. WALKER, and A. S. WELANDER
General Atomics, P.O. Box 85608, San Diego, California 92186-5608

†*Triniti Laboratory, Troitsk, Russia*

Received August 19, 2004
Accepted for Publication March 25, 2005

The integrated plasma control approach provides a systematic method for designing plasma control algorithms with high reliability and for confirming their performance off-line prior to experimental implementation. This approach includes construction of plasma and system response models, validation of models against operating experiments, design of integrated controllers that operate in concert with one another as well as with supervisory modules, simulation of control action against off-line and actual machine control platforms, and iteration of the design-test loop to optimize performance. Using this approach, required levels of robustness to model uncertainties and off-normal events can be quantified and incorporated in the design process. The DIII-D digital plasma control system (PCS) enables application of this method by providing a flexible programming environment and an architecture for real-time parallel operation of a set of computers that executes the large set of control algorithms needed for exploration of the advanced tokamak regime. The present work describes the DIII-D PCS and the approach, benefits, and progress made in integrated plasma control as applied to the DIII-D tokamak, with implications for the International Thermonuclear Experimental Reactor design and other next-generation tokamaks.

KEYWORDS: *plasma control, tokamak control, MHD stabilization*

I. INTRODUCTION

The most demanding plasma control requirements of DIII-D are driven by the need to support the development and exploration of the advanced tokamak (AT) regime,[1] an essential part of the DIII-D scientific mission. ATs are characterized by a high degree of shaping, achievement of profiles optimized for high confinement and stability characteristics, and active stabilization of magnetohydrodynamic (MHD) instabilities to attain high values of normalized beta and confinement. Achieving and sustaining such performance requires extremely accurate regulation of the plasma boundary; active control of internal profiles, pumping, fueling, and heating; as well as simultaneous and coordinated MHD control action to stabilize such instabilities as tearing modes and resistive wall modes (RWMs). High performance in the AT regime typically requires operation near stability boundaries for these modes, as well as for the vertical instability (made more virulent by the high elongation required for high beta). This demanding task of simultaneous and accurate operating point regulation and stability control action requires a high degree of integration in both the design process and operation of the plasma control system (PCS). These requirements will be even more critical in tokamaks operating in a burning plasma regime due to the potentially destabilizing effects of the fusion self-heating, the need to control additional quantities (e.g., heat loads), and the more serious consequences of control failure.

Advanced tokamaks operate in narrow windows of physics operating space in order to achieve high performance. These windows of operating space are characterized by a high degree of coupling among configuration, choice of operating point, transport, and stability. Figure 1 illustrates many of the important transport couplings within tokamak plasmas. In order to sustain high AT performance, plasma equilibria must be held in a

*E-mail: humphreys@fusion.gat.com

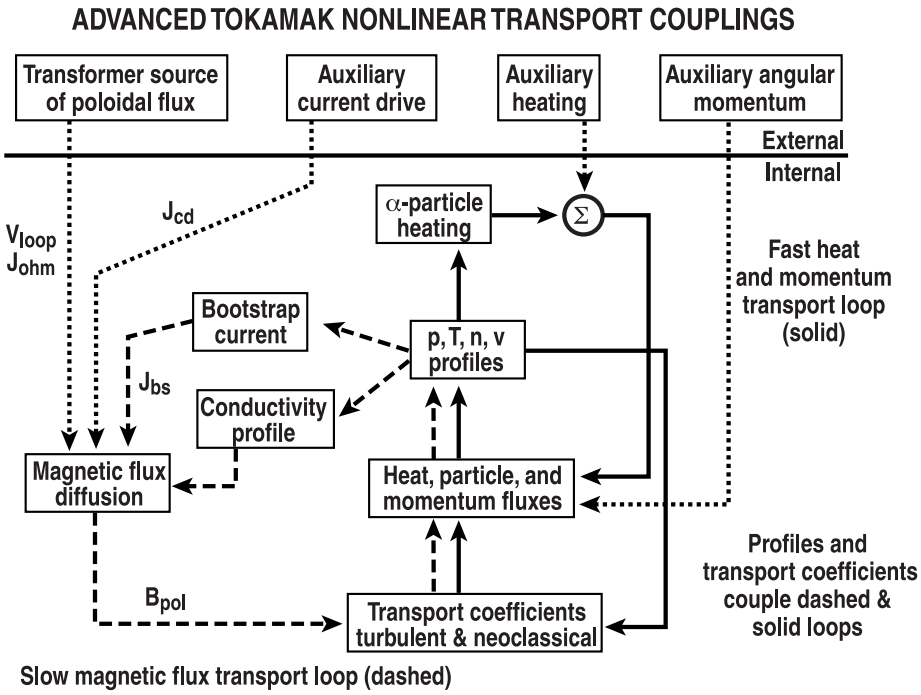

Fig. 1. A schematic of some of the relationships between highly coupled physics effects in ATs. V_{loop} = loop voltage, J_{Ohm} = ohmic current density, J_{cd} = auxiliary current drive density, J_{bs} = bootstrap current density, and B_{pol} = poloidal magnetic field. P, T, n, and v refer to plasma pressure, temperature, density, and velocity, respectively.

highly optimized shape. Current and pressure profiles must be maintained in a form characterized by good bootstrap current alignment and actively driven noninductive current. Internal transport barriers must also be maintained, and a variety of MHD instabilities must be suppressed. Figure 2 shows the set of actuators used to achieve this integrated control on DIII-D with high performance in AT regimes. The large set of 18 poloidal field (PF) shaping coils located relatively close to the plasma allows highly accurate control of equilibria with a high degree of shaping (access to high PF multipole moments). Heating is primarily provided by a 20-MW neutral beam system. Current can be driven by a 3-MW electron cyclotron current drive (ECCD)/electron cyclotron heating (ECH) gyrotron system.[2] Density and divertor performance are regulated by a combination of position control and a set of divertor cryopumps.[3] Disruption effects can be mitigated by the use of high-pressure impurity injection, which terminates the discharge without conducted thermal flux to the divertor and without runaway electron production.[4]

The use of any individual actuator in the system can strongly affect more than one physics response, so accurate descriptions of the cross coupling of these effects must be built into models of the system in order to design high performance controllers. The availability of theory-generated models themselves is not sufficient, however. In order to provide operational confidence and quantifiable controller reliability, models used for control design must also be validated extensively across a broad range of operating regimes. Once such sufficiently accurate dynamic models of system responses have been validated against experimental data, a rich array of computational tools is available for design of controllers. Linear multivariable design techniques, for example, allow explicit design for desired performance and enable the determination of controllers without the necessity of empirical optimization, which traditionally consumes extensive machine operation time. Approaches such as linear optimal design[5] allow weighting of the desired relative importance of actuator power and control error accuracy, while H_∞ (Ref. 6) and other robust design methods allow shaping of control loop response while ensuring specified robustness to nonideal effects such as model uncertainties. For present-day devices, the use of such design techniques can greatly reduce the need for machine time for testing and optimization and can even allow determination of high-reliability controllers prior to ever producing the target equilibrium experimentally.

Control design is typically based on simplified system models that are often linearizations of explicitly nonlinear processes. Controller performance must be tested against more realistic simulations prior to implementation, particularly to assess performance in the presence of actuator saturation, power supply nonlinearities, nonlinear plasma response, and other complex system details.

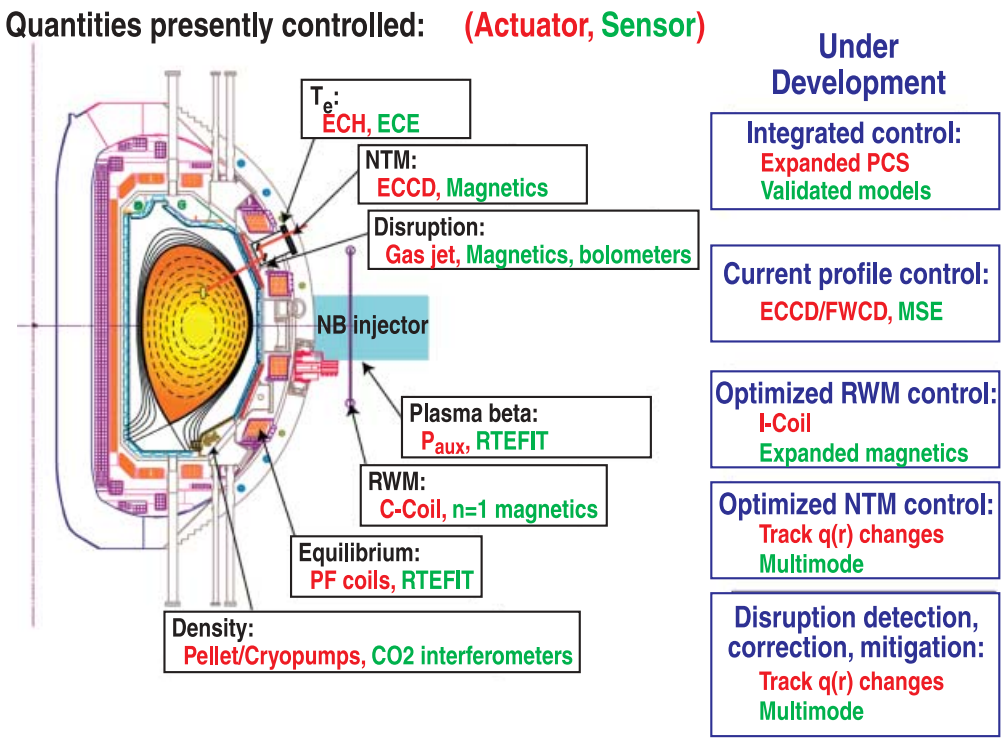

Fig. 2. A schematic representation of DIII-D control actuators and sensors.

Integrated plasma control requires two different kinds of simulation: "off-line" testing of controllers implemented in a simulation and "hardware-in-the-loop" testing of the PCS controller implementation running on actual real-time computers communicating with the simulation. Hardware-in-the-loop simulations verify both the correctness of the controller implementation in the PCS and the performance of the algorithm itself under realistic hardware and system response conditions (for example, network and CPU intercommunication).

We refer to the design and testing process that makes use of validated control-level models for performance-based design and confirms performance in both off-line and hardware-in-the-loop simulations as "integrated plasma control." Control-level models ideally contain the minimal level of detail required to describe the relevant control problem and often include linearized representations of intrinsically nonlinear processes. The integrated plasma control approach is particularly important in design and analysis of control schemes, controllers, and implementations for next-generation devices such as the International Thermonuclear Experimental Reactor (ITER). Well before the start of operations in a new device, the various elements of the integrated control approach allow determination of the performance expected along with related engineering consequences. Using this approach, control schemes and detailed algorithms can be designed and thoroughly tested prior to machine operation and will provide high performance control with high confidence. The need for experimental testing and consumption of machine time in early operational use of such controllers is therefore greatly reduced. The complete array of elements of this design approach now in operational use at DIII-D comprises a unique and complete integrated plasma control tool set for design and commissioning of such high reliability control.

The present work describes the application of integrated plasma control techniques to DIII-D and draws implications for ITER and other next-generation devices. Section II describes the nature of the control problem in ATs. Sections III and IV describe the DIII-D PCS and integrated plasma control tools in use at DIII-D, along with examples of application to axisymmetric and non-axisymmetric control. Section V discusses implications for ITER, and concluding comments are made in Sec. VI.

II. CONTROL ISSUES IN ATs

Regulation of the operating point in an AT typically includes maintaining a high degree of shaping, providing axisymmetric stability control typically operating near performance limits, sustained profile control, as well as active heating and density control. AT reactors will need to maintain this narrow operating window in the presence of alpha-particle heating and the potential for thermal

runaway. Constraints on steady-state shape regulation are severe for a reactor, which can tolerate only momentary excursions from the nominal equilibrium, and are often in partial conflict with the design pressures of the demanding AT configuration. For example, high performance AT equilibria must have high elongation, leading to high vertical instability growth rates. The natural response to fluctuations in such a plasma, typically operating near the ideal vertical stability limit, produces high frequency fluctuating fields at the PF coils. However, the superconducting PF coils of a reactor place strong restrictions on the amplitude of these fluctuating fields because of the resultant alternating-current loss heating, which can quench the coils.

An AT must also provide passive and/or active MHD stability control in order to achieve and sustain high values of normalized beta. One method of MHD stability control is to ensure good operating point control since regulation of selected profile characteristics can maintain equilibria at operating points that are stable to various MHD modes. For example, local current drive or heating to modify plasma profiles may allow maintenance of the jump in flux-normalized flux gradient

$$\Delta' \equiv \frac{1}{\psi}\frac{d\psi}{dr}\bigg|_{r=r_s-\varepsilon}^{r=r_s+\varepsilon}$$

(evaluated at the resonant surface location $r = r_s$) sufficiently negative to stabilize the neoclassical tearing mode[7] (NTM). An alternative approach is to allow fundamentally unstable equilibria but provide active stabilization of the resulting MHD modes. For example, driving current at the location of NTM islands can completely stabilize these modes.[7] Alignment of the current drive deposition region with the location of the island can require plasma positioning, toroidal field control, or launcher articulation control with precision and accuracy of ~1 to 2% relative to the minor radius (equivalent to ~1 to 1.5 cm in DIII-D). Satisfying such dynamic control constraints in the presence of typical disturbances and noise in an AT plasma requires taking into account the effect of various control loops on NTM control action. If control of the plasma position with respect to the divertor pumping location is used for density control, this must be integrated with the NTM control in order to synchronize divertor pumping and mode suppression. Active alignment of ECCD deposition and the target rational q surface must also be continued following mode suppression in order to account for changes in the q profile that result from the improved performance.

Stabilization of the RWM can also increase the achievable normalized beta.[8] Systematic design methods can aid in optimizing RWM control algorithms that drive nonaxisymmetric coils so as to oppose the kink displacement of a growing RWM. Such methods can also aid in design of algorithms for filtering diagnostic array data to discriminate between true RWMs and other nonaxisymmetric phenomena such as edge localized modes, which can erroneously be interpreted by the control system as a growing RWM (Ref. 9). Stabilization of these and other MHD modes can lead to different profiles and therefore different dynamic responses. These variations should then be accounted for in the MHD suppression as well as in coupled equilibrium and profile control in order to sustain robust stabilization.

III. THE DIII-D PCS

The DIII-D PCS (Ref. 10) provides an extremely flexible environment in which to develop and implement control algorithms and fully supports the integrated plasma control approach. It has been recently upgraded with commercial off-the-shelf components, including a cluster of nine CPUs running in parallel with low-latency (10 μs) packet-switched Myrinet® network communication. The PCS is fully scalable, allowing easy extension of performance by adding more processors to existing computers or more computers to the entire system. Use of multiple parallel computers allows many control loops to execute simultaneously, each with access to the full speed of each CPU, but with the capability of different update time intervals.[10] A Myrinet® network switch coordinates data transfer among computers to efficiently exploit this asynchronous parallel architecture. Figure 3 summarizes the architecture schematically. Data are acquired using 32-channel D-TACQ® digitizers capable of up to 250-kHz sampling rates. The DIII-D PCS performs all aspects of conventional tokamak plasma control, regulating equilibrium shaping, density, stored energy, and plasma current, among other operating point characteristics.[11] Equilibrium control is provided through real-time solution of the Grad-Shafranov equation to determine flux errors at the plasma boundary and divertor strike points and field errors at the X point(s) via the RTEFIT algorithm.[12] Equilibrium control is performed on several different cycle times, ranging from 50 μs for vertical stability control to 3.5 ms for the slowest boundary control loop corresponding to the fully updated real-time equilibrium reconstruction time. However, more rapid shape control is concurrently produced on a 250-μs cycle time using partially updated equilibrium reconstructions. Density control is accomplished through regulation of a combination of gas puffing and strike-point position relative to a cryopump plenum. Control of the total stored energy is achieved through modulation of the neutral beams.[13] Feedback control of radiation from the plasma has been demonstrated using measurements of bolometer and impurity line radiation to regulate impurity gas puff and divertor cryopumping rates.[3] All of the algorithms described above routinely make use of proportional-integral-derivative feedback laws, although the PCS also provides and makes use of multivariable state space-described feedback laws

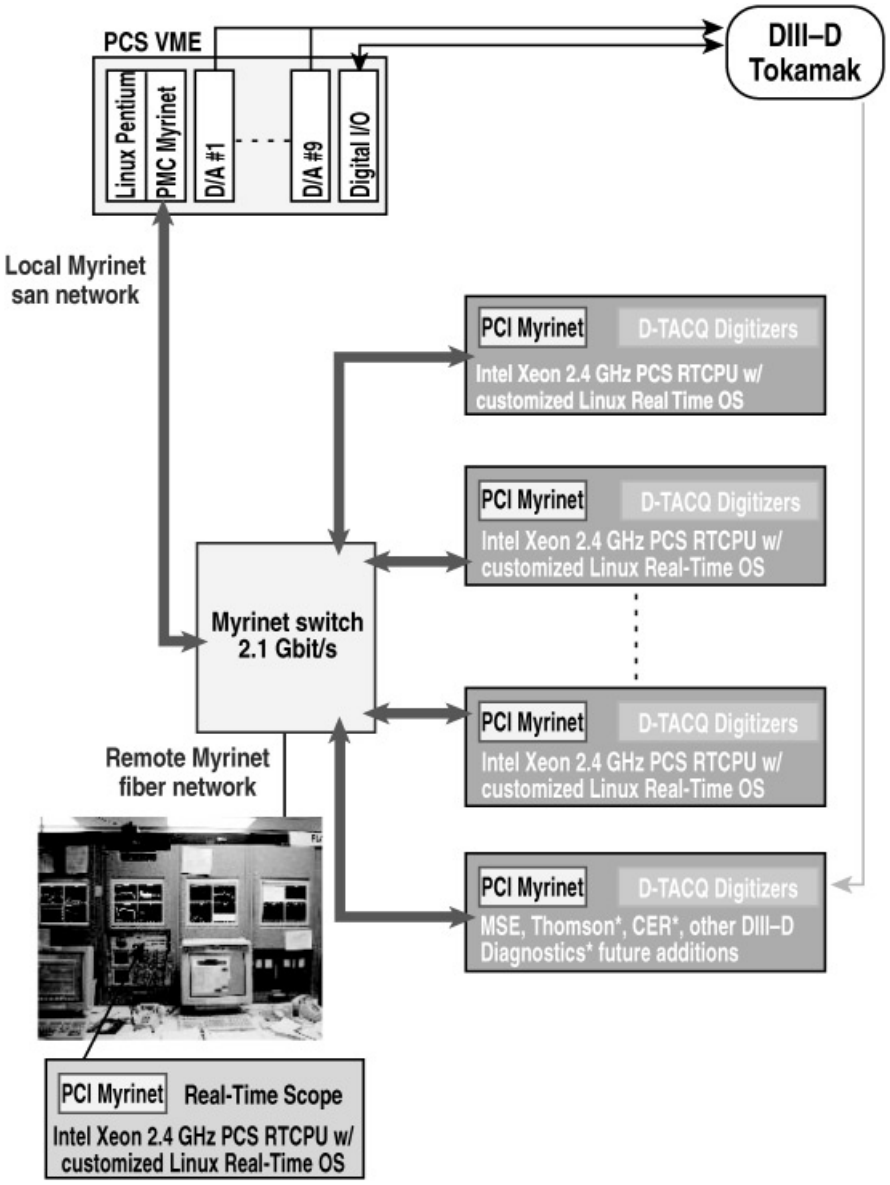

Fig. 3. DIII-D PCS architecture and hardware characteristics. The remote Myrinet® optical fiber network allows computer/digitizer combinations to be located throughout the facility and in particular where diagnostic signals are available. 32-channel, 250-kHz sampling rate D-TACQ® digitizers are used to acquire data.

for more complex control applications, which are used less frequently.

The demands of AT operation beyond conventional tokamak plasma control are also satisfied by the DIII-D PCS. Several MHD instabilities that are highly unstable in DIII-D AT regime operation are explicitly stabilized through PCS control action, including the vertical instability, RWM, and NTM. Error field control is performed by the PCS through preprogrammed or active feedback regulation of currents in ex-vessel (C-coil) or in-vessel (I-coil) nonaxisymmetric coil sets.[14] Real-time ion cyclotron resonance frequency antenna loading control is accomplished by regulating the outboard gap between antenna and separatrix.[15] Real-time calculation of the safety factor profile has recently been implemented in the PCS, using a separate real-time computer to execute the RTEFIT algorithm including motional Stark effect (MSE) measurements of the PF. This capability is a first step toward achieving real-time current profile control in DIII-D using ECCD (Ref. 16) and fast-wave current drive as actuators.

The DIII-D PCS operating system is Linux based but customized to run without interrupts while performing control so that 100% of the CPU is dedicated to the

real-time process. The PCS software infrastructure has been designed to be generic and can be used as the basis for a PCS on any tokamak.[17] For example, the software kernel of the DIII-D PCS is now in use on the NSTX (Ref. 18) and MAST (Ref. 19) devices and is being similarly adapted[20] for use on both the KSTAR (Ref. 21) and EAST (Ref. 22) superconducting ATs presently under construction.

IV. INTEGRATED PLASMA CONTROL IN DIII-D

Integrated plasma control as used here refers primarily to a methodology for systematically developing and confirming the performance of multivariable controllers, which must function with high reliability in a tightly coupled environment. This approach is summarized schematically in Fig. 4. The flow of logic begins with physics understanding (a), which produces models of system response (b) that are used in the design of control algorithms (c). Typically models used in control design must be linearized or otherwise simplified from the full nonlinear physical response of the system. These "control-level" models are usually quite different from the detailed physics models and simulations used to broadly understand fundamental principles at work in a tokamak. Linearized models in particular allow use of the rich technology of linear multivariable control design to produce robust and/or cost-functional optimized controllers. The resulting control designs are then tested against detailed system simulations (d), which include important nonlinearities such as actuator or sensor saturation and the full range of nonlinear plasma responses, and allow iterative improvement of controller performance. Optimized controllers are then implemented in the control software running on the actual control computer hardware (e), and the software implementation is tested against the detailed system simulation (d). This hardware-in-the-loop test confirms that the implementation is correct and that no unforeseen functional details of the control hardware will adversely affect control operation. It also confirms that control performance is satisfactory under a range of plasma conditions that represents the expected space of operation and that may correspond to significantly nonlinear perturbations from the design operating point. A critical element of the process is to ensure that experimental results are used at the beginning of the process and continuously through operation to validate the models used for design and simulation.

This process is essential for commissioning and operating high performance tokamaks and will be particularly important for reactors with demanding nuclear licensing constraints. The key elements are high reliability (validated) models of all parts of the system response, a highly detailed simulation environment that can be used to test controllers either off-line or connected with the actual plasma control computer hardware, and a flexible PCS that can support all aspects of the design process. We now examine these elements in detail.

IV.A. Axisymmetric System Models and Control

Integrated plasma control that simultaneously regulates and stabilizes the various elements of DIII-D must take into account the coupling among the various physics phenomena. The many different system models required to describe this coupling include the axisymmetric equilibrium and plasma profile evolution in response to conductor currents; plasma response to current drive, heating, and particle source actuators; and MHD stability response to the relevant actuators (e.g., ECCD in the case of NTM suppression, nonaxisymmetric magnetics in the case of RWM stabilization). Modeling of axisymmetric

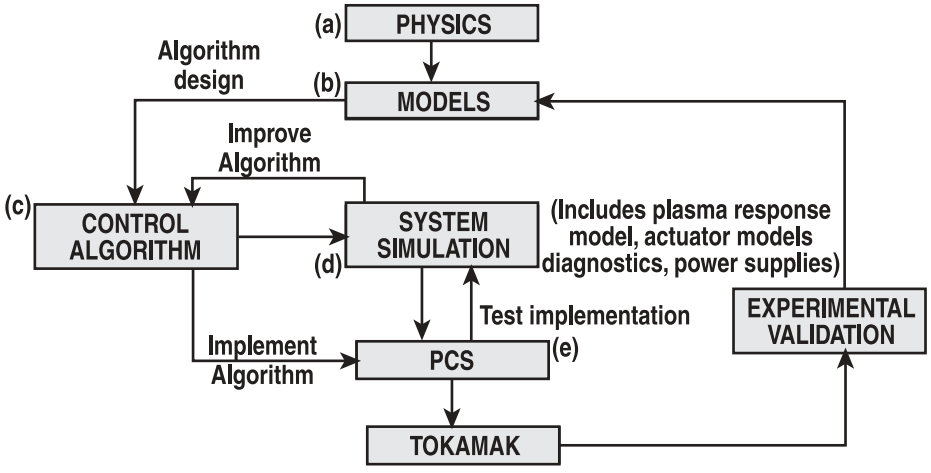

Fig. 4. Elements of the integrated plasma control approach.

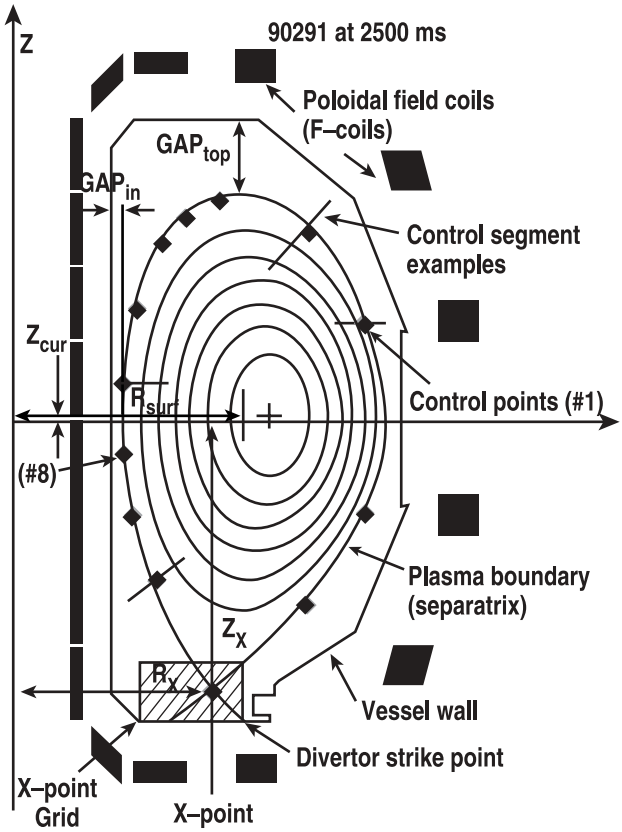

Fig. 5. DIII-D cross section and control segments and points of the isoflux boundary shape control scheme.

equilibrium evolution with constrained profiles has been very successful over the past decade. Early and powerful work with simple current- or flux-conserving rigid plasma displacements has led to nonrigid plasma models, which best match experimental responses when the PF over the plasma cross section is approximately conserved rather than conserved in detail. Such models have successfully reproduced detailed plasma evolution in several experiments and have enabled design of multivariable controllers, which have been tested successfully in experimental devices.[23,24]

The success of partial rather than detailed flux conservation constraints in modeling plasma responses suggests that the finite resistivity of a tokamak plasma plays a significant role, as has long been suggested.[25] The dynamic response of edge currents, in particular, is strongly affected by the relatively high resistivity of the edge plasma. In DIII-D, currents driven in the edge plasma region (with $T_e \sim 100$ to 500 eV) typically diffuse with time constants on the order of 5 to 20 ms, comparable to shape and position control timescales. These timescales are much shorter than the core plasma current diffusion time (many seconds in DIII-D), which is the relevant timescale roughly accounted for in approximate flux-conserving plasma models. Ignoring edge current dynamics in the DIII-D plasma model can have a particularly dramatic effect on shape and stability control performance owing to the use of the "isoflux" control scheme. This scheme seeks to make the flux at a set of specified locations, which are required to be on the boundary, equal to the flux value at the X point (or the limiter touch point). In order to control the shape of the plasma boundary in detail consistent with the high multipole moments produced (in principle) by the coil set, the DIII-D PCS typically regulates (in the case of a single null divertor, for example) a set of 13 control points along with X-point radial and vertical positions[10] (Fig. 5). The explicit control of flux values at many points on the nominal plasma boundary (in contrast with control of plasma boundary shape parameters, for example) means the details of the flux response can be particularly critical to good performance. Accordingly, the linear response models used for design under the DIII-D control scheme need to include the effects of both nonrigid and resistive plasma dynamics, particularly in the edge region, in order to allow accurate control design.

Development of a nonrigid, resistive axisymmetric plasma model parallels the familiar derivation of general axisymmetric plasma response models. These models of shaping and stability response are typically based on a combination of Faraday's law applied to toroidal conductor circuits and perturbed plasma equilibria or simple force balance equations.[26] The general form of the resulting conductor circuit equation for linearized plasma displacements is

$$M_{ss}\dot{I}_s + R_{ss}I_{ss} + M_{sp}\dot{I}_p + \frac{\partial\psi_s}{\partial\xi_R}\dot{\xi}_R + \frac{\partial\psi_s}{\partial\xi_Z}\dot{\xi}_Z = V_s \ , \quad (1)$$

and a resistive plasma can be included in the overall circuit equation via

$$M_{pp}\dot{I}_p + R_{pp}I_p + M_{ps}\dot{I}_s + \frac{\partial\psi_p}{\partial\xi_R}\dot{\xi}_R + \frac{\partial\psi_p}{\partial\xi_Z}\dot{\xi}_Z = 0 \ , \quad (2)$$

where

I_s = vector of perturbed conductor currents

I_p = vector of perturbed plasma fluid element currents

V_s = vector of perturbed conductor voltages

ψ_s = vector of perturbed flux at conductors

ξ_R, ξ_Z = plasma fluid element major radial and vertical displacement vectors, respectively

R = resistance matrix

M = mutual inductance matrix

p,s = subscripts that denote plasma and stabilizing conductors, respectively.

It is common to neglect plasma inertia by ordering the timescales of interest to be much longer than the Alfvén time (a valid assumption for long-wavelength MHD modes mediated by resistive structural elements), so that the plasma can be taken to be in quasi equilibrium at all times. Under this massless-plasma assumption, the linearized radial (F_R) and vertical (F_Z) force balance at each fluid element are given, respectively, by

$$\delta F_R = 0 = \frac{\partial F_R}{\partial I_s} I_s + \frac{\partial F_R}{\partial I_p} I_p + \frac{\partial F_R}{\partial \xi_R} \xi_R + \frac{\partial F_R}{\partial \xi_z} \xi_z + \frac{\partial F_R}{\partial \beta_p} \beta_p \quad (3)$$

and

$$\delta F_Z = 0 = \frac{\partial F_Z}{\partial I_s} I_s + \frac{\partial F_Z}{\partial I_p} I_p + \frac{\partial F_Z}{\partial \xi_R} \xi_R + \frac{\partial F_Z}{\partial \xi_z} \xi_z + \frac{\partial F_Z}{\partial \beta_p} \beta_p \ , \quad (4)$$

where β_p is a perturbed poloidal beta (scalar or vector representing local values). Combining Eqs. (1) through (4) produces a cumulative circuit equation describing toroidal conductors and plasma fluid element currents and includes the effect of nonrigid plasma displacement under the massless or quasi-equilibrium assumption. The plasma current vector I_p is often determined by either fixing it (constant current approximation), varying the I_p values in order to exactly conserve flux at each element (exact ideal MHD approximation), or conserving some measure of average flux over the plasma (approximate flux conservation). Because most forms of this latter constraint conserve flux according to a weighting that emphasizes the core, it can represent an approximation to the dissipative effect of a resistive edge. We explicitly include a plasma circuit equation such as Eq. (2) (which allows each fluid element current to vary according to the local neoclassical resistivity) to account for resistive magnetic flux diffusion through the plasma even more accurately, provided the plasma resistivity is sufficiently well known.

Figure 6 shows a high-order eigenmode of the perturbed plasma current profile in DIII-D, calculated using the dynamics described by Eqs. (1) through (4). The mode is distinctly different from a uniform change in current. In particular, the inboard-outboard asymmetry of the eigenmode reflects its strong coupling to major radial motion of the plasma. Figure 7 shows displacement vectors for a distinctly nonrigid eigenmode of plasma motion, corresponding to an expansion of both inboard and outboard midplane gaps. As in the case of Fig. 6, this mode is significantly different from a rigid radial or vertical mode. Using a rigid model to represent the plasma response would thus produce poor control of such a mode. Good dynamic control of the edge with controllers derived from a plasma response model requires inclusion of such effects in the model.

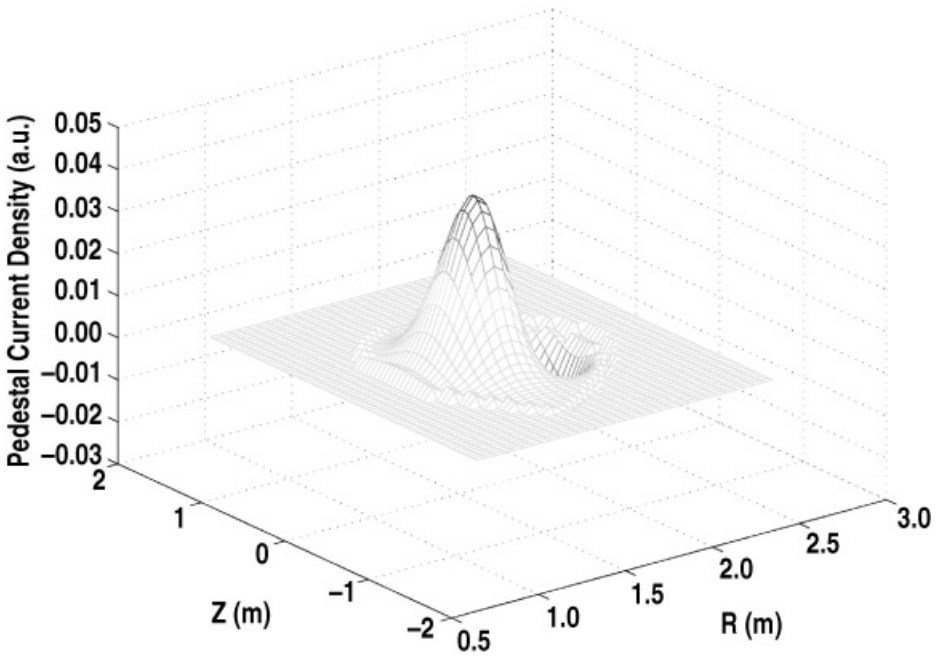

Fig. 6. The calculated response of a resistive plasma current corresponding to a major radial motion is very different from a uniform current variation mode.

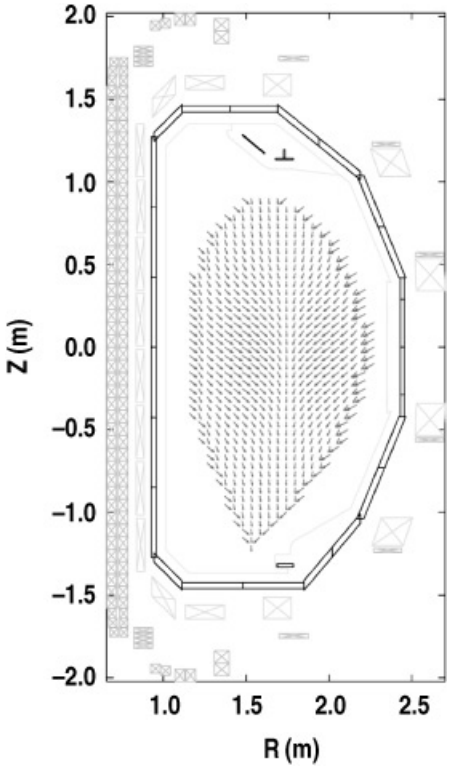

Fig. 7. The calculated nonrigid plasma response corresponding to expansion of both inner and outer gaps. This response mode must be accounted for in modeling to produce good control design.

Given accurate axisymmetric plasma models, linear multivariable [multiple input/multiple output (MIMO)] control design techniques can produce controllers that explicitly take into account performance requirements, such as the trade-off between shape accuracy and PF coil voltage or current demand. Several such controllers have been designed and experimentally implemented on DIII-D (Ref. 23). However, nonlinear limits intrinsic to the operation of DIII-D require nonlinear control approaches. One such class of limits arises from the need to make best use of the large set of "chopper" switching regulators and coils on DIII-D, often resulting in coil currents approaching one of two operating limits during the evolution of a discharge. Allowing the current to fall close to 0 may produce a "latched-on" condition in the chopper resulting in a coil current that does not respond to the command signal. This typically ends the discharge. Similarly, attempting to exceed 2500 A in a chopper will result in an overcurrent limit "trip," which shuts down the chopper entirely, again often terminating the discharge. Avoiding these limits in developing a new discharge type can require iterative adjustment of control gains between boundary flux errors and a corresponding coil demand by control system operators. Producing a linear MIMO controller predictively requires either a similar iteration (in simulation) to avoid these limits or a real-time nonlinear algorithm that seeks to prevent approaching limits too closely. Such nonlinear limit-avoidance algorithms have been designed, and initial implementation and testing has begun on DIII-D (Ref. 27). In order to prevent such limiting, the control system replaces the actual shape error signal with the best approximation to this signal under the constraint that it will not cause the coil currents at steady state to exceed their limits. Figure 8 shows a comparison of two simulations: one in which a linear shape controller determines the shape evolution without constraint and one in which an online optimization is performed as well to replace the measured error with a constrained error signal to avoid coil current limits while still providing satisfactory equilibrium control. In Fig. 8a, several selected coil currents are shown driven to limiting values by the linear controller in the absence of current limiting logic (dashed lines). Although the same limiting behavior occurs in many coil currents in the simulation, only a few are shown for clarity. In actual operation, this behavior would have caused a chopper to latch and ended the plasma discharge. The solid lines show prevention of this behavior in the presence of the limit-avoidance algorithm. Figure 8b shows the penalty on isoflux control point flux errors resulting from avoiding current limits (solid) relative to allowing the limits to be exceeded (dashed). Again only a few representative flux errors are shown, although similarly large divergence occurs in virtually all of the control points as a result of the coil current limiting. Figure 8c shows similar effects on X-point position control. Significant but acceptable deviations from the target values are seen in both control point flux error and X-point position errors as a trade-off for avoiding coil current limits and likely discharge termination.

IV.B. Off-Line and Hardware-in-the-Loop Simulations

The final element of the integrated plasma control development process is simulation of control function to confirm performance. Testing of control algorithms against detailed simulations constructed of well-validated modules allows assessment of control algorithm performance under more realistic (e.g., nonlinear) conditions prior to implementation in the tokamak PCS. Such off-line simulations are particularly important when the control design is carried out with linear or otherwise simplified models, yet the final system contains important nonlinearities and other complexities not well described by the design-level models. Figure 9 shows a schematic of a highly integrated simulation, including axisymmetric control elements (for example, a plasma-conductor model such as the DINA nonlinear $1\frac{1}{2}$D resistive MHD code[28]), MHD control elements (NTM and RWM), and disruption detection/mitigation elements. Each loop contains detailed representations of both controllers and physics response models and can include complex logic as well

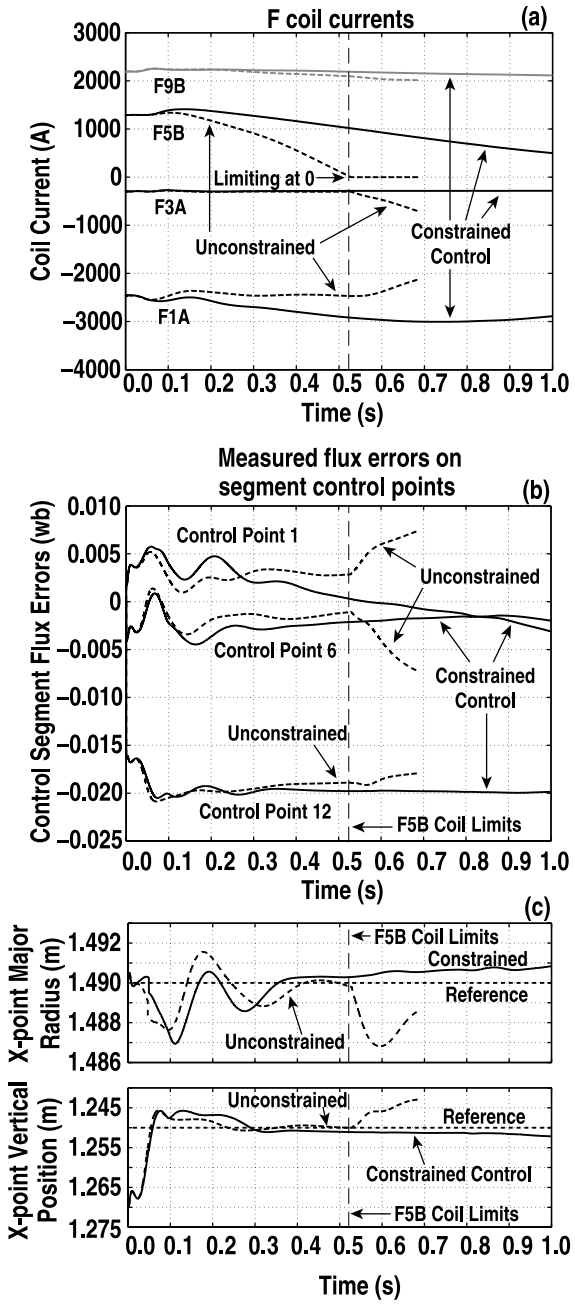

Fig. 8. Simulations illustrating action of a coil current limit-avoidance algorithm: Individual coil current limits are avoided at the cost of some shape/position control accuracy. (a) Currents in four different shaping coils (dashed = unconstrained, solid = constrained); (b) flux errors at three different boundary control points; (c) X-point major radial and vertical position (short dashes = reference values).

as mathematical signal processing operations. For off-line simulations, the controller representation includes all important aspects of the DIII-D PCS, including computational and data-transfer latencies, antialiasing filter dynamics, and dynamics associated with the PCS algorithms themselves. A detailed schematic of the axisymmetric core of the simulation is shown in Fig. 10. It includes models of direct-current power supplies, fast switched power supplies, field shaping and ohmic heating coils, vacuum vessel, linear plasma response, data filters, magnetic diagnostics and analog to digital (A/D) and digital to analog (D/A) signal converters. Either linearized plasma models such as that described in Sec. IV.A or a detailed nonlinear model such as the DINA code[28] can be used for the plasma block. These models have been validated against DIII-D experimental data in significant detail.[29]

Confirmation of the controller implementation on the actual control hardware is obtained through the hardware-in-the-loop simulation process. This step involves directly running the actual PCS hardware and software implementation of control algorithms against detailed simulations similar to those used for off-line simulation. Summarized schematically in Fig. 11, hardware-in-the-loop capability is an integral part of the DIII-D PCS. The PCS ordinarily receives input directly from tokamak diagnostics while sending out actuator control signals to the various control subsystems. The simulation is designed to provide modeled diagnostic signals exactly paralleling the set of signals obtained from the tokamak in experimental operations. The PCS then performs its real-time calculations and outputs the resulting actuator commands. Event timing between simulation and PCS matches the timing experienced in experimental operations as well. This allows testing of such hardware-dependent characteristics as calculation delay, data-transfer latency, signal-to-port alignment, filter performance, and network communication. This final testing step provides high confidence in implementation and controller performance under realistic machine operational conditions well before experimental execution.

IV.C. Development of NTM Suppression Algorithms with Integrated Plasma Control

Integrated plasma control has been extensively applied to the design and development of DIII-D NTM suppression algorithms. Use of this systematic design method was largely responsible for the successful suppression of the 3/2 NTM in first-time use of these active control algorithms.[7] Alignment of ECCD current with the location of an NTM island allows replacement of the bootstrap current deficit, which characterizes the instability. The NTM control system in DIII-D includes two coupled algorithms for achieving the necessary alignment of the NTM island and the ECCD deposition region: the Search and Suppress and Active Tracking routines. These algorithms can regulate either the plasma major radial position, the toroidal field, or the plasma vertical position in order to produce sufficient alignment of the island and ECCD deposition location. In broad

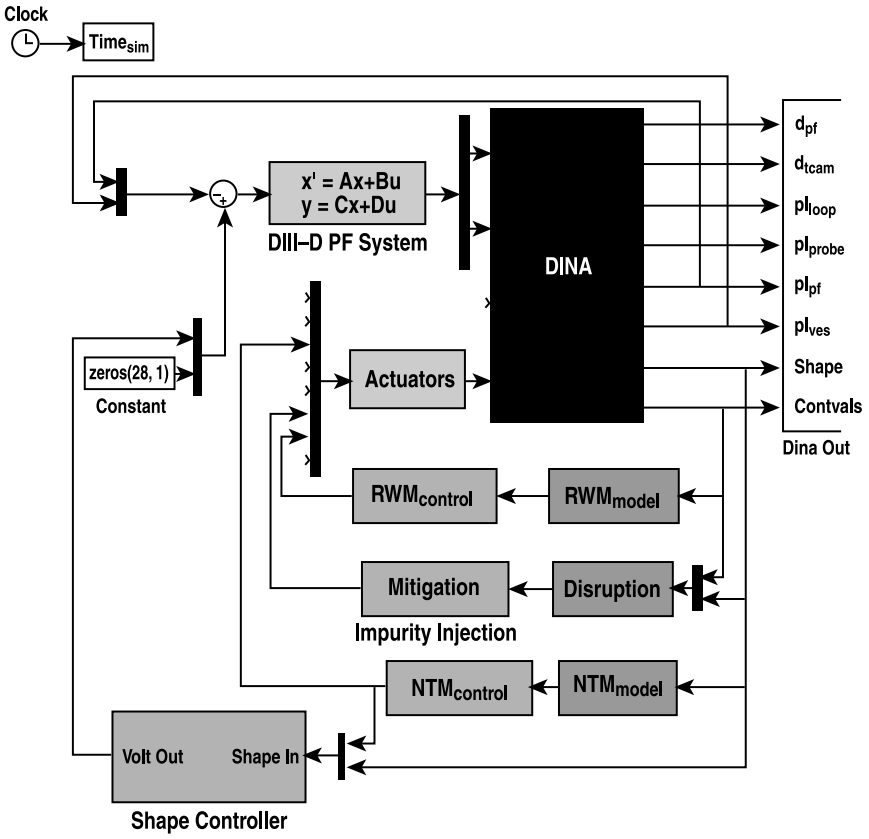

Fig. 9. The off-line integrated simulation includes both axisymmetric and nonaxisymmetric MHD control elements for study of multiple simultaneous control functions.

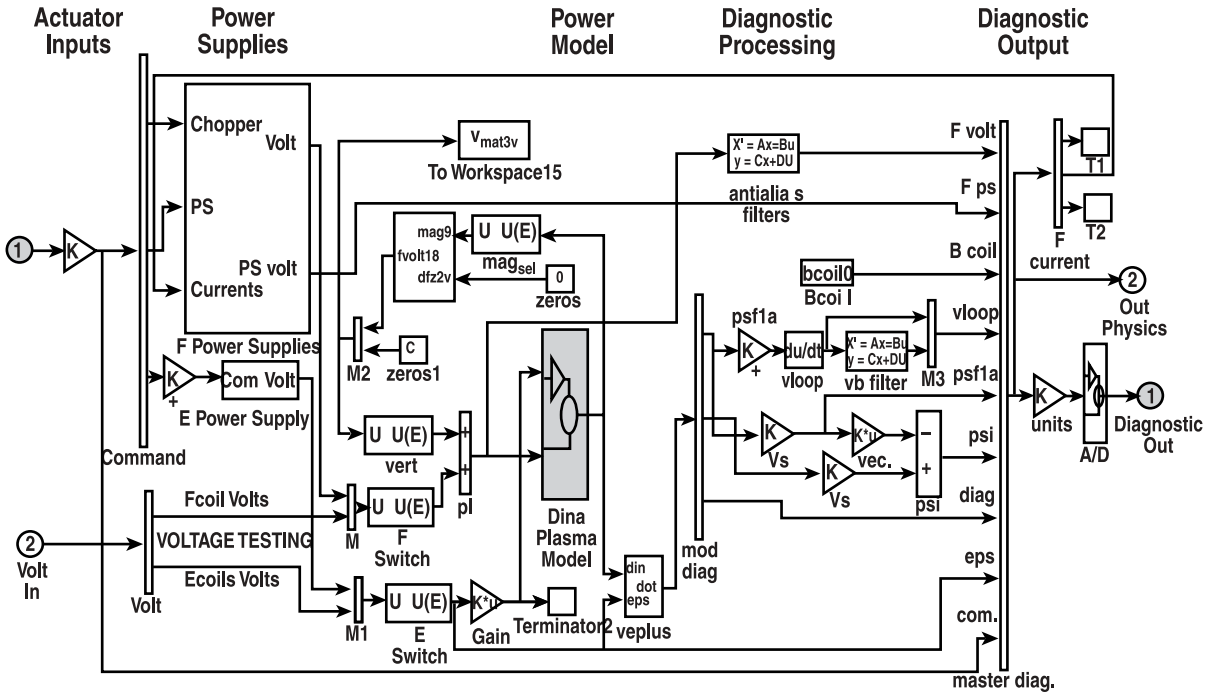

Fig. 10. Elements of the DINA/DIII-D axisymmetric system simulator, used for both off-line and hardware-in-the-loop simulation.

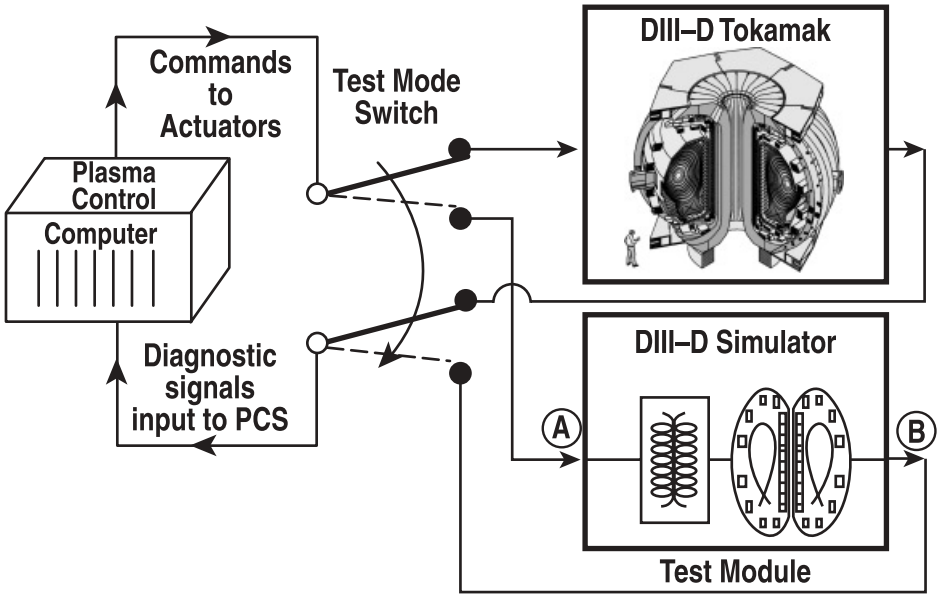

Fig. 11. Hardware-in-the-loop schematic. Actual plasma control computer hardware and controller implementations can be operated against the DIII-D simulator test module instead of the tokamak itself.

terms, the Search and Suppress algorithm performs a scan of one of these control quantities in discrete steps, with pauses to assess the effect on the island size (inferred from the root-mean-square amplitude of high frequency magnetic measurements). If the present value of the control quantity produces a satisfactory rate of reduction in island size, the algorithm holds that position until the island is suppressed or the island size saturates at a finite amplitude. Insufficient suppression results in continued searching within a specified range of values of the control quantity. Successful suppression results in a freeze of the control quantity and an activation of the Active Tracking algorithm. This algorithm is needed to maintain island/ECCD alignment after the mode has disappeared since there is no longer any overt magnetic signature to reflect the degree of alignment. The Active Tracking algorithm uses a nonlinear predictor based on static magnetic measurements to estimate the degree of misalignment. Several predictors are available to the routine, but the most accurate calculation results from use of Adaptive Learning Network predictors.[30] These networks are a class of neural networks based on piecewise-linear basis functions rather than the more familiar Gaussian (radial) or sigmoidal basis functions. All predictors implemented in the PCS are trained on previous experimental discharge data or artificially generated data to produce an estimate of the position of the relevant flux surface relative to the plasma geometric centroid. If toroidal field control is being used, the required toroidal field correction is derived from the calculated major radius correction command.

The many control parameters defining the dynamic function of the NTM suppression algorithm were determined using the integrated plasma control process. Two different models were used in this development. A nonlinear model of the island response to ECCD current was developed based on a simplified version of the modified Rutherford equation[7] (MRE). Simulations were then developed incorporating the simplified model or highly detailed implementations of the MRE, in which some physics quantities were identified from previous DIII-D experimental data. Figure 12 shows a comparison of the mode suppression model and the experimental response to variation in the degree of alignment between island and ECCD location (Fig. 12a, dashed line labeled "Simulated"). The model island response dynamics are easily accurate enough for good control design. In the case shown, the plasma major radius (Fig. 12b) was varied to adjust the alignment of the island flux (safety factor $q = 1.5$) surface with the ECCD deposition location. The signature of Active Tracking, enabled to compensate for variations in the $q = 1.5$ surface due to changes in the current profile and poloidal beta, can be seen in the fluctuating major radius perturbations following suppression at $t \sim 3.4$ s.

The result of using the Search and Suppress with Active Tracking in an experimental application can also be seen in Fig. 12. At the initial misalignment of 1.5 to 2 cm, the ECCD produces a slowing in the growth of the mode but not suppression of the island size. The major radius is adjusted by the Search and Suppress to produce sufficient alignment to fully suppress the mode within 200 ms. To accommodate common DIII-D operating constraints, the NTM control algorithm is integrated with a special plasma shape/position regulation scheme that fixes the strike points when the major radius is varied to adjust the island/ECCD alignment. This allows for constant

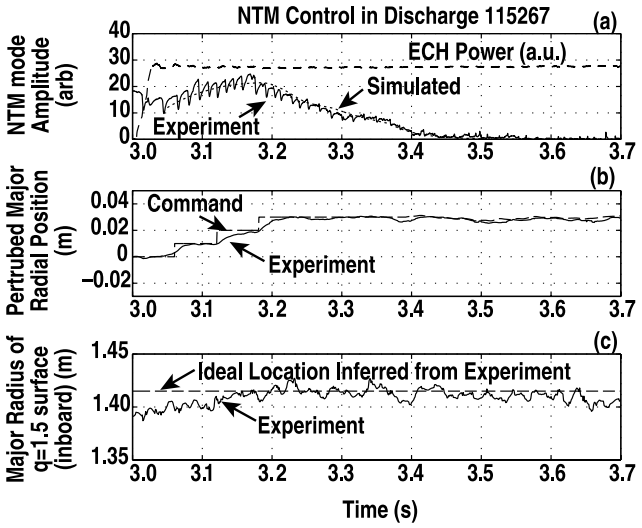

Fig. 12. NTM suppression experiment and simulation using design model of island response to ECCD application: (a) NTM mode amplitude, (b) perturbed major radial position, and (c) major radius of $q = 1.5$ surface (inboard).

divertor pumping[13] while NTM suppression is performed. Using integrated plasma control techniques, the NTM control algorithm was designed with sufficient reliability to produce successful suppression and tracking of the evolution of the profile to maintain island/ECCD alignment the first time this integrated active suppression was attempted experimentally.

V. INTEGRATED PLASMA CONTROL AND ITER

The ITER device design poses significant challenges to control design and operation.[31] Many of these challenges are unique owing primarily to its role as a burning plasma experiment. Regulation of the divertor leg position, for example, must be achieved with better than 1-cm accuracy, with severe constraints on allowable transient violation of shape and position control. The ITER reference configuration is lower single null, but flux expansion near the upper X point can produce significant scrape-off layer heating of the upper first wall region with even small excursions from the reference configuration. In later phases of operation, ITER is expected to operate in an AT mode beyond the no-wall beta limit using active RWM and NTM stabilization, high performance shaping control, and active profile control.[32] Both the demanding elements of long-pulse operation and the substantial alpha-particle self-heating will further complicate the multivariable coupled control problem. Long-pulse operation, with discharge lengths of many current diffusion times, can exacerbate the control problem by introducing significant drift in the magnetic and other integrated diagnostic signals, which are key to accurate shape and profile control. The fusion self-heating can lead to thermal runaway and must be actively regulated and integrated with other operating point control actions. The neutron flux associated with significant fusion power can also induce stray voltages in superconducting coils, which may affect the control action in complex ways.

Detailed modeling and simulation to ensure that control performance is adequate prior to use in actual operations will be essential in commissioning the ITER PCS. Indeed, the nuclear nature of the ITER plant makes it likely that such performance confirmation will be a licensing requirement. Elements of the integrated plasma control approach have been applied to ITER control design and analysis, but end-to-end design and performance confirmation tools for ITER are still in early stages of development.[33,34] Work has begun to apply the full integrated plasma control approach to ITER axisymmetric control design and performance confirmation using the DIII-D PCS hardware-in-the-loop capability. A detailed axisymmetric simulation of the ITER system was developed, based on models extensively validated on DIII-D. An ITER PCS was then constructed based on software from the DIII-D PCS and was run in closed loop with the ITER model in hardware-in-the-loop simulation mode to study realistic gap responses to initial perturbations. Figure 13 shows a simulated system response to an initial perturbation in the vertical position, including the effects of actual hardware signal and computation delays. This disturbance scenario represents a loss of vertical control. The gaps (Fig. 13a) are restored to their unperturbed values within 2 s with a plasma current perturbation of <60 kA (Fig. 13b), while the vertical position overshoot is $<20\%$ of the initial displacement (Fig. 13c). The simulation shows good performance (although not optimized in this case) in the presence of

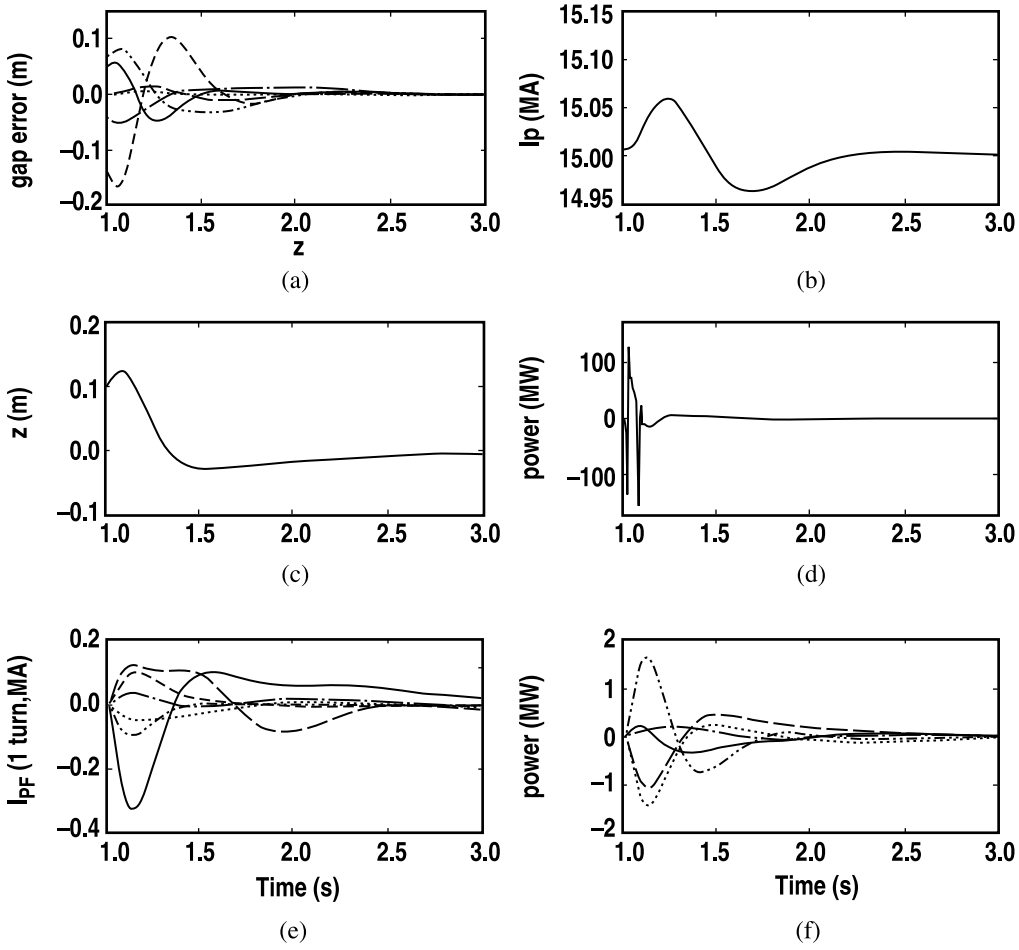

Fig. 13. Integrated plasma control hardware-in-the-loop simulation of ITER gap control demonstrates good response after initial loss of vertical control in presence of actual hardware and computational delays: (a) gap errors, (b) plasma current, (c) vertical position, (d) power consumption, (e) PF coil current perturbations, and (f) central solenoid segment current perturbation.

actual hardware and computational delays. This end-to-end process shows the power of the approach and demonstrates the readiness of presently available tools to address the control design and commissioning needs of ITER and other next-generation devices.

VI. SUMMARY AND CONCLUSIONS

The integrated plasma control approach provides a systematic method for developing high reliability control systems for ATs. This approach is highly efficient, allowing development of high confidence, high performance control algorithms with greatly reduced need for experimental testing and optimization time. The approach has been extensively applied to DIII-D, and elements have been applied to other tokamaks around the world as well as in design projects for next-generation devices such as ITER. Present-day devices exploring the AT regime have produced sufficient physics understanding to enable accurate modeling of many of the critical response elements. However, the increasing need for accurate models to produce high reliability control highlights the important role of presently operating machines in the design of next-generation devices. In exploring high performance AT regimes, devices such as DIII-D are producing the models needed for design of these new machines. DIII-D has also become a rich test bed for development of advanced plasma control methods themselves. The DIII-D PCS provides a highly flexible environment that supports all aspects of the integrated plasma control approach, including testing of PCS hardware and software against detailed simulations. Increasingly, experimental successes in performance enhancement on DIII-D, through sustained operation in AT regimes, are being made possible through detailed modeling, simulation, control design, and algorithm improvement performed prior to actual experimental use. Successful application of such coupled

control algorithms upon first-time use in DIII-D has demonstrated the reliability and importance of the integrated plasma control approach for next-generation device designs as well.

ACKNOWLEDGMENTS

This is a report of work supported by the U.S. Department of Energy under cooperative agreement DE-FC02-01ER54698. The authors are grateful for the kind contribution of Fig. 1 by P. A. Politzer of General Atomics.

This paper summarizes the work done by the DIII-D program in this area over the past 20 yr or more and includes the contributions of many members of the DIII-D Team listed in the Appendix of this volume of *Fusion Science and Technology*.

REFERENCES

1. J. R. FERRON et al., in *Proc. 29th Conf. Plasma Physics and Controlled Fusion*, Montreux, Switzerland, 2002, Vol. 26B, P1.060, European Physical Society (2002).

2. R. W. CALLIS et al., in *Proc. 20th Symp. Fusion Technology*, Marseille, France, 1998, Vol. 1, p. 315, Association EURATOM-CEA, Saint-Paul-Lez-Durance (1999).

3. G. L. JACKSON et al., *J. Nucl. Mater.*, **241–243**, 618 (1997).

4. D. G. WHYTE et al., *Phys. Rev. Lett.*, **89**, 55001 (2002).

5. J. M. MACIEJOWSKI, *Multivariable Feedback Design*, Addison-Wesley, Wokingham, England (1989).

6. D. C. McFARLANE and K. GLOVER, *Robust Controller Design Using Normalized Coprime Factor Plant Descriptions*, Springer-Verlag, Lecture Notes in Control and Inf. Sci., **138** (1989).

7. R. J. LA HAYE et al., *Phys. Plasmas*, **9**, 2051 (2002).

8. A. M. GAROFALO et al., *Phys. Plasmas*, **6**, 1893 (1999).

9. C. M. FRANSSON, D. G. EDGELL, D. A. HUMPHREYS, and M. L. WALKER, "Model Validation, Dynamic Edge Localized Mode Discrimination, and High Confidence Resistive Wall Mode Control in DIII-D," *Phys. Plasmas*, **10**, 3961 (2003).

10. B. G. PENAFLOR, J. R. FERRON, R. D. JOHNSON, and D. A. PIGLOWSKI, in *Proc. 4th IAEA Technical Mtg. Control, Data Acquisition, and Remote Participation for Fusion Research*, San Diego, California, 2003, *Fusion Eng. Des.* (to be published).

11. M. L. WALKER, D. A. HUMPHREYS, and E. SCHUSTER, in *Proc. 16th IEEE/NPSS Symp. Fusion Engineering*, Champaign, Illinois, 1995, Vol. 2, p. 885, Institute of Electrical and Electronics Engineers (1996).

12. J. R. FERRON et al., *Nucl. Fusion*, **38**, 1055 (1998).

13. T. S. TAYLOR et al., in *Proc. 14th Int. Conf. Plasma Physics and Controlled Nuclear Fusion Research*, Würzburg, Germany, 1992, IAEA-CN-56/A-3-1, International Atomic Energy Agency (1992).

14. J. T. SCOVILLE and R. J. LA HAYE, *Nucl. Fusion*, **43**, 250 (2003).

15. G. L. CAMPBELL et al., in *Proc. 17th Symp. Fusion Technology*, Rome, Italy, 1992, p. 1017, Elsevier Science Publishers B.V. (1993).

16. J. LOHR, in *Proc. 27th Int. Conf. Infrared and Millimeter Waves*, San Diego, California, 2002.

17. J. R. FERRON, B. G. PENAFLOR, M. L. WALKER, J. MOLLER, and D. BUTNER, in *Proc. 16th IEEE/NPSS Symp. Fusion Engineering*, Champaign, Illinois, 1995, Vol. 2, p. 870, Institute of Electrical and Electronics Engineers (1996).

18. E. J. SYNAKOWSKI, in *Proc. 19th IAEA Fusion Energy Conf.*, Lyon, France, 2002, OV/2-2, International Atomic Energy Agency (2002).

19. B. LLOYD, in *Proc. 19th IAEA Fusion Energy Conf.*, Lyon, France, 2002, OV/2-3, International Atomic Energy Agency (2002).

20. J. A. LEUER et al., "DIII-D Integrated Plasma Control Tools Applied to Next-Generation Devices," *Proc. 23rd Symp. Fusion Technology*, Venice, Italy, Sep. 2004, *Fusion Eng. Des.* (submitted for publication).

21. D. I. CHOI et al., in *Proc. 17th IEEE/NPSS Symp. Fusion Engineering*, Vol. 1, p. 215, Institute of Electrical and Electronics Engineers (1997).

22. Y. X. WAN, in *Proc. 19th IAEA Fusion Energy Conf.*, Lyon, France, 2002, FT/P2-03, International Atomic Energy Agency (2002).

23. M. L. WALKER et al., in *Proc. 21st Symp. Fusion Technology*, Madrid, Spain, 2000.

24. M. ARIOLA et al., *Fusion Technol.*, **36**, 126 (1999).

25. T. H. JENSEN and F. W. McCLAIN, *J. Plasma Phys.*, **32**, 399 (1984).

26. D. A. HUMPHREYS and I. H. HUTCHINSON, *Fusion Technol.*, **23**, 167 (1993).

27. M. L. WALKER, D. A. HUMPHREYS, and E. SCHUSTER, in *Proc. 42nd IEEE Conf. Decision and Control*, Maui, Hawaii, 2003, 6565, Institute of Electrical and Electronics Engineers.

28. R. R. KHAYRUTDINOV and V. E. LUKASH, *J. Comput. Phys.*, **109**, 193 (1993).

29. J. A. LEUER et al., in *Proc. 20th Symp. Fusion Engineering*, San Diego, California, 2003.

30. D. O. GORODNICHY, W. W. ARMSTRONG, and X. LI, Lecture Notes in Computer Science, Vol. 1311, *Proc. 9th Int. Conf. Image Analysis and Processing (ICIAP '97)*, Florence, Italy, Vol. II, p. 332 (1997).

31. A. PORTONE et al., *Fusion Technol.*, **32**, 374 (1997).

32. R. AYMAR et al., *Nucl. Fusion*, **41**, 1301 (2001).

33. R. ALBANESE et al., *Fusion Technol.*, **30**, 167 (1996).

34. M. L. WALKER, D. A. HUMPHREYS, and E. SCHUSTER, in *Proc. 20th Symp. Fusion Engineering*, San Diego, California, 2003.